

Test Results for HINS SSR2 Focusing Lens

J. DiMarco, E. Khabiboulline, M. J. Kim, F. Lewis, C. Hess, D. F. Orris, M. Tartaglia, I. Terechkine, T. Wokas

Table of Contents

- 1. Introduction**
- 2. Test Overview**
- 3. Quench Training History**
- 4. Quench Data vs. Model Analysis**
 - A. Configuration 1**
 - B. Configuration 2**
 - C. Configuration 3**
 - D. Configuration 4**
 - E. Error Analysis**
 - F. Inductance and Resistance Analysis**
 - G. Optimal Quench Protection Configuration**
- 5. Modeling Temperature Decay**
- 6. Magnetic Measurements**
- 7. Summary**
- 8. References**

1. Introduction

The SSR2 focusing lens was designed for the high energy section (60-100 MeV) of the HINS R&D front end proton linac. It consists of two identical main coils (MC) bordered on the ends by two identical bucking coils (BC), along with corrector coils located radially inward. Fig. 1-1 provides a schematic of this solenoid, whose detailed design is described in [1]. Two other focusing solenoid development and test programs for the lower energy (CH, SSR1) sections of HINS were completed; the SSR2 is considered the most challenging due to the larger stored energy and potentially damaging high voltages and temperatures that could result during a quench; thus significant effort was devoted to modeling quench development and optimizing the quench protection scheme. A prototype magnet (SS2_Sol_01d) was built, and although the HINS program was subsequently terminated, testing of this device and validation of model predictions was still of interest for applications, such as ProjectX front end design [2].

In addition to the quench performance issues, alignment of the solenoid magnetic axis is also an important concern. The four-coil system, with each wound on a separate bobbin and later assembled around a common beam tube, could complicate the magnetic axis position determination and reproducibility. Therefore some study of the solenoid axis has been made at various stages of the construction and testing.

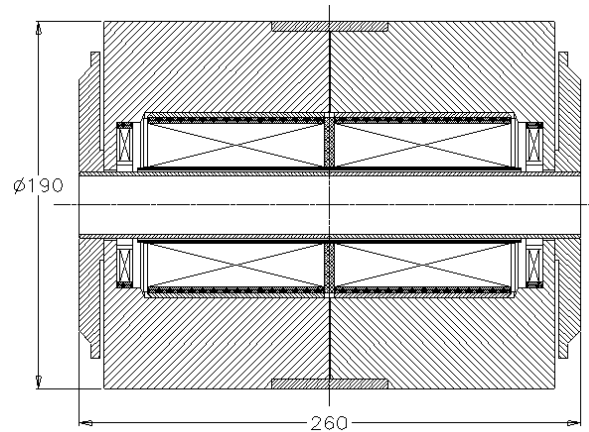


Fig. 1-1. SSR2 focusing lens design concept.

2. Test Overview

Testing was conducted in the IB1 Magnet Test Facility on stand 3 in February 2012. After the initial installation a set of warm magnetic measurements was made to verify proper coil polarities, and in fact they were found to be incorrect – a dangerous situation for the magnet because the main coils would repel each other with very large force. This was corrected and polarities were again checked before the first cool down on 2/29 to liquid helium temperature; the cold magnet then passed a hipot of 500 Volts to ground. The test plan consisted of solenoid quench training, during which four different dump resistor protection configurations were investigated (these are described in detail in section 4); in order to achieve this, each of the splices between coils was also connected to a power lead (in addition to the two main leads connecting to the power supply, or five leads total). One pair of leads was available to connect both dipole correctors in series to a separate power supply. Quench performance of the correctors (powered in series) was measured first with the solenoid off, then in the solenoid field at its nominal operating current (200A); magnetic measurements of the solenoid and correctors were made. The test was completed on March 26, 2012.

The test took nearly a month to complete due to an unusually large number of data acquisition and power system problems that affected testing. Some of these issues are relevant to understanding the quench data (in case of future study): some issues with isolation amplifiers resulted in saturated voltage signals, intermittent large voltage offsets on some signals, and lost coil voltage data for one quench event. There are indications (including some from a previous magnet test) that the magnet current measurement is distorted just after the dump fires; a sharp 15% current drop in ~ 3 ms is not understood, and is also not consistent with coil voltage signals. The cause is under investigation.

3. Quench Training History

The solenoid quench history is summarized in Fig. 3-1 and described in detail here. The quench training was started using the first protection scheme, in which 1.3Ω resistors were connected across the terminals of each MC; for this case the dump switch was delayed by 1

second to allow all energy to be dissipated in these resistors and the quenching coils. After a dozen training quenches the magnet achieved a reasonably high current, and the second resistor configuration was tested, with $1\ \Omega$ across each MC and $3\ \Omega$ across each BC; the solenoid was then trained to the expected plateau current of 242 A. In fact in the two quenches at this highest current (#15,#18), the quenches originated in a MC, and shortly thereafter a quench started in a BC. Some retraining appears to happen after thermal cycles, and in general the quench training is somewhat erratic – the solenoid did not consistently reach the expected plateau. After quench #21 the third protection scheme was implemented, using a $3\ \Omega$ dump resistor across the entire magnet with a dump switch enabled. As discussed below, a fourth scheme, with no protection resistor, was inadvertently tested as well.

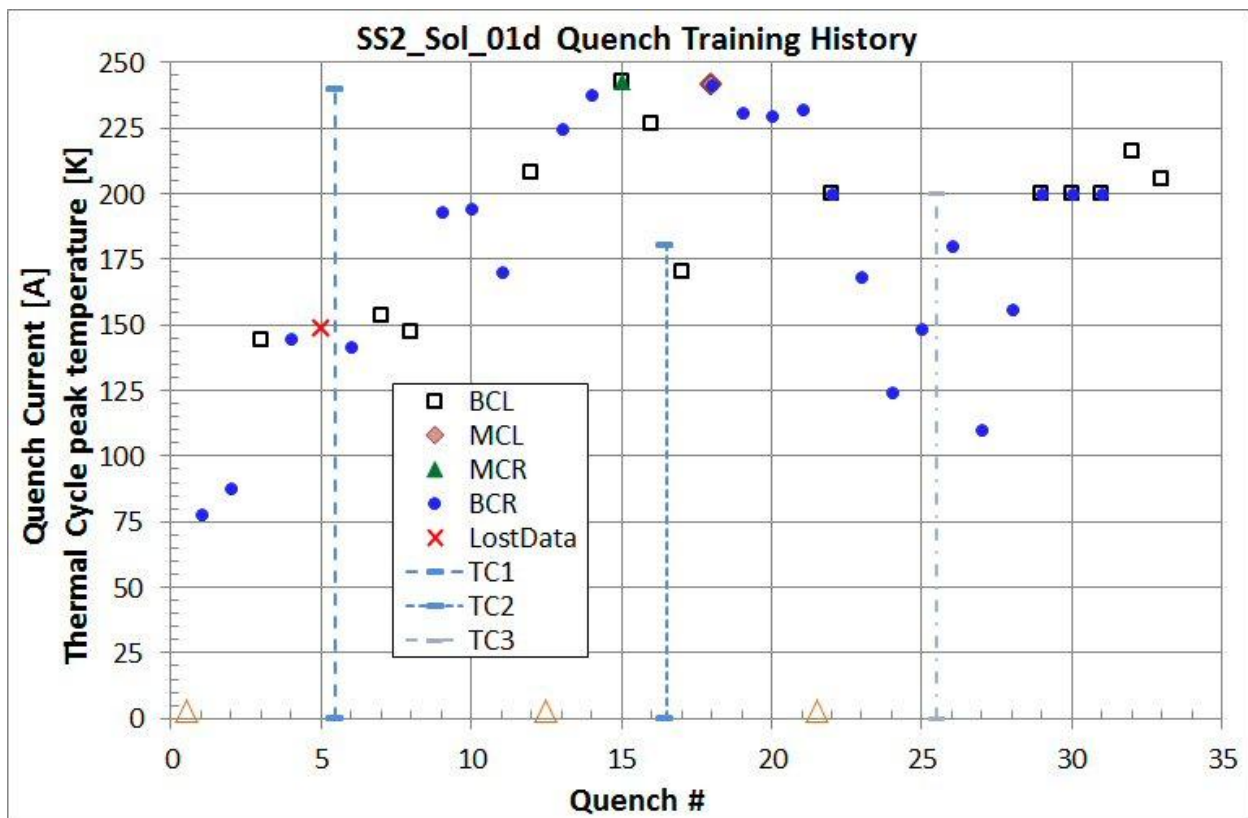


Fig. 3-1. Quench training history of the SSR2 solenoid. Open triangles on horizontal axis indicate changes of the protection resistor configuration, as described in section 4.

At this point, dipole corrector-only training was performed, and two successive Horizontal Dipole (HD) quenches occurred at 143 A. Next the solenoid was powered to 200 A and the Vertical dipole (VD) quenched at 47.8 A, which is the expected short sample limit. In all of these cases, the quench started in one dipole and soon after the other dipole also quenched; this is expected because the small 0.25 mm insulation layer between windings allows the quench to propagate radially. The dipole quench detection by a separate Analog Quench Detection (AQD) module causes the dump to fire without delay, and the resulting rapid current decay

induced quenches in both bucking coils (#22). In subsequent ramps to repeat this test, the solenoid was very erratic, but eventually it reached 200 A; however the system tripped due to copper lead signal (Cu-I) imbalance, causing the dump to fire without delay and again quenching both BCs (#29). Quench #30 again resulted from a trip – due to a large coil inductive voltage excursion caused by rapidly changing current - while starting to ramp the dipoles with the solenoid at 200 A. *It was then realized that the dump switch delay was actually still set to 1 second (an oversight by the operating physicist)*, thus inadvertently causing the solenoid stored energy to be internally dissipated during quenches #23-28, and #30 (configuration 4). Finally (#31), with the solenoid at 200 A, the dipoles quenched again at 47.8A with exactly the same pattern of VD then HD quench development, and both solenoid BCs quenched during the rapid current decay.

Two final solenoid quenches were made with the proper 10 ms dump delay, and the test was ended when further erratic behavior was seen. When the magnet was removed from the test stand, *it was found that several of the bolts through the yoke - which provide pre-stress on the coil system – had worked themselves loose during the quench testing* (they had been properly torqued prior to the test). This offers a reasonable explanation (coil motion due to inadequate mechanical support) for the erratic quench behavior in the latter part of the test; another hypothesis, that temperatures in the BCs could remain elevated for a long time when the entire stored energy is dissipated in the solenoid, seems highly unlikely in view of results from quench and thermal modeling (discussed in section 4). *Nevertheless, future versions of the design must include measures to prevent this!*

4. Quench Data vs. Model Analysis

To reiterate, quench protection of the HINS SSR2 solenoid is of primary interest. By detailed study of the quench data and we can learn about how the focusing lens reacts to quenching and whether the proposed quench protection schemes function as predicted by computational models. Over the course of testing, the following four lens configurations were investigated:

1. 1.3 ohm resistors connected in parallel with main coils.
2. 1 ohm resistors connected in parallel with main coils and 3 ohm resistors connected in parallel with bucking coils.
3. 3 ohm resistor connected in series with focusing lens.
4. No protection (zero resistance connected in series with focusing lens).

We selected and analyzed one quench event from each of the above configurations to determine the effectiveness of each quench protection scheme and compared experimental results with the predictions of computational modeling of quench propagation. It is notable that *in almost all cases, the unquenched BC becomes resistive shortly after quench detection as the current rapidly decays*; therefore it is an important aspect to include in modeling the system for comparison to the data. Three versions of the modeling program exist for the HINS SSR2 system:

Model 1: An older version which only allows for quenching in one coil and can model only case 1 (see [3]).

Model 2: A newer version which can model case 1 (see [4]) and case 2 (see [5]), and which provides extended capabilities, such as more accurate modeling of the magnetic field in the lens and the ability to allow for multiple quenching coils.

Model 3: A version optimized to model cases 3 and 4, with resistance in series to the lens.

The events selected for analysis are essentially the highest current quenches for each case, but in which only a single coil quenches (until detection time when current begins to decay). The very highest current events (at the critical surface) are more complex and show quenches developing in both MC and BC prior to detection; we felt that it is not a good case for comparison to model since there may be some other resistance growth hidden by the large inductive voltages. Also, we are most interested in protection at operating current – which is lower – and in which the quench origin – the worst case – is most likely only in one coil. Events in which the dipole coils were powered were also not considered since the model does not include this additional field.

4. A) Configuration 1: 1.3 Ohm Resistors in Parallel with Main Coils

First, it is useful to examine how the system behaves as a function of current, to try to understand whether it is important to make simulations at different current levels. Figures 4-1 and 4-2 show that the peak voltages developed in the first and second quenching BCs are quite linear in the range of currents where we observed quenches. At low current, the behavior should be slightly non-linear (V must go to zero as I goes to zero), and there is probably a threshold current below which the spectator BC does not quench during the rapid current decay. Given the observed linear behavior at high current, simulation of a single high current quench is sufficient.

We compare model predictions for this configuration to data from quench event #12, with 208.1 A maximum current and initiation in the lead end bucking coil. The observables we have available to compare are the total solenoid current and individual voltages across each of the coils, each as a function of time. Test data for coil temperatures could not be collected, so one relies completely on the model to predict the thermal behavior during a quench.

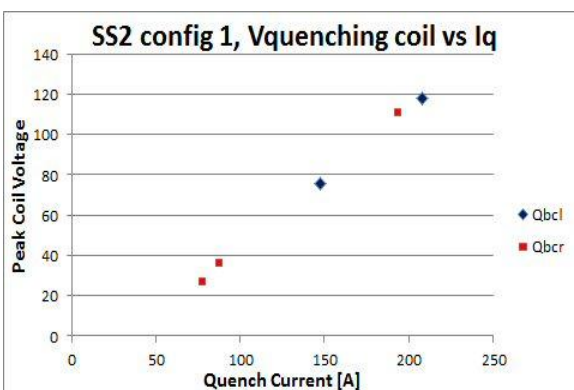


Fig. 4-1. Peak voltage across initially quenching bucking coil vs. quench current.

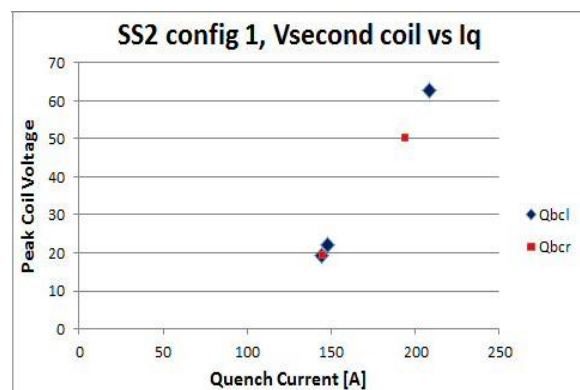


Fig. 4-2. Peak voltage across second bucking coil vs. quench current. Blue: Lead end

Trends indicate the same behavior independent of which BC initially quenches. bucking coil quenches initially. Red: Return end bucking coil quenches initially.

First, we simulate a single bucking coil quench using Model 1: Figures 4-3 and 4-4 illustrate the current decay and voltages across coils, for both data and model. The experimental and modeled current decay graphs match up well, except for initially faster decay predicted by the model. However, the voltage graphs (Fig. 4-4) differ greatly. In general, the model predicted much higher voltages (by as much as 120 V) across the coils than occurred in the actual quench event.

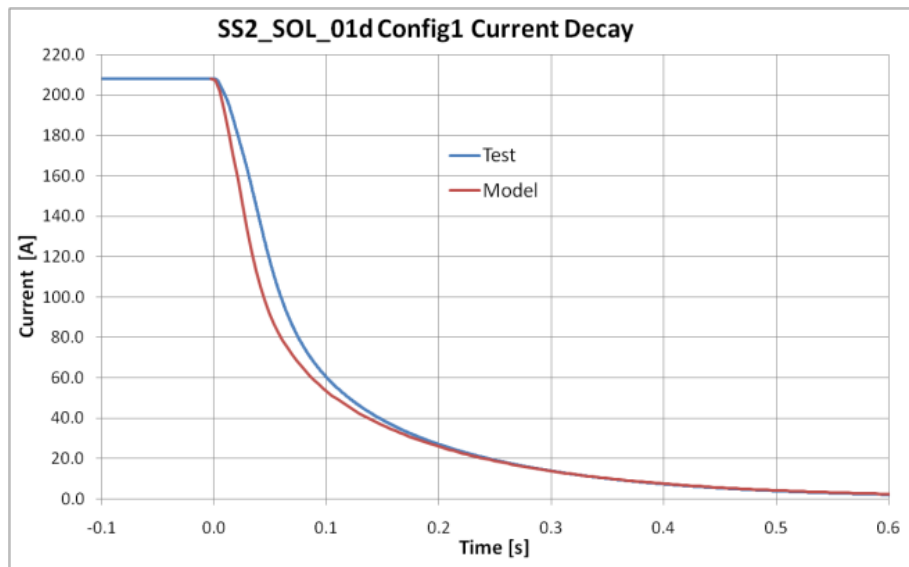


Fig. 4-3. Current vs. time for Configuration 1, Test data and Model 1 result (only initial bucking coil quench developed).

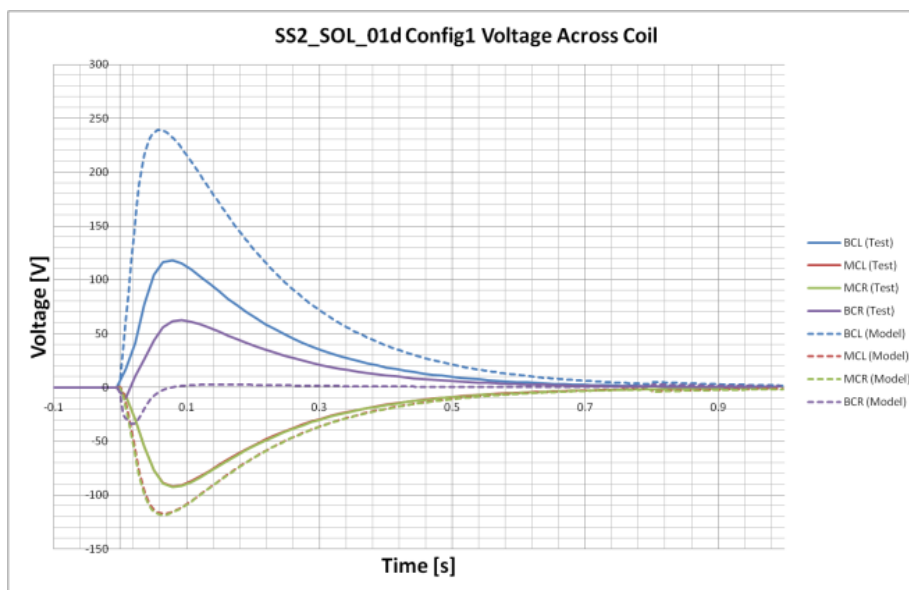


Fig. 4-4. Voltage across coils vs. time for Configuration 1. Test data (solid lines) and Model 1 result (dashed lines), only initial bucking coil quench developed.

This disparity is not too surprising, since conservative assumptions made in the model tend to overestimate conditions in the coil; e.g., quench propagation is modeled assuming isothermal conditions, with quench originating in the high field region. Moreover, faster current decay corresponds to higher voltages. Still, the discrepancy is quite large and is qualitatively wrong for the second bucking coil: It is clear that a secondary quench occurred in the return end bucking coil at approximately 12 ms after the initial quench. The developed resistance would explain the high positive voltage in the return end bucking coil as well as the generally lower voltages throughout the system, since energy dissipation would be more evenly distributed in the lens.

Running Model 2 to simulate the case of just a single BC quench gave results equivalent to those of Model 1, thus providing some verification. Model 2 was run again with the same parameters, except that a quench was initiated in the return end bucking coil (BCR) 12 ms after the first BCL quench. Fig. 4-6 and Fig. 4-7 provide the current and voltage graphs for this modeled case with dual quenching, superimposed on test data.

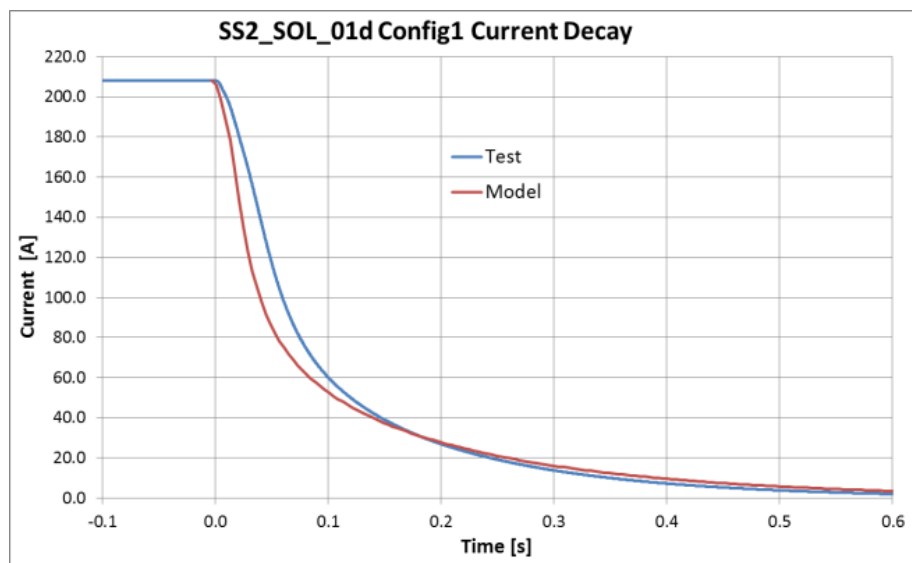


Fig. 4-5. Current vs. time for Configuration 1, Test data and Model 2 result (second bucking coil quench developed after 12 ms).

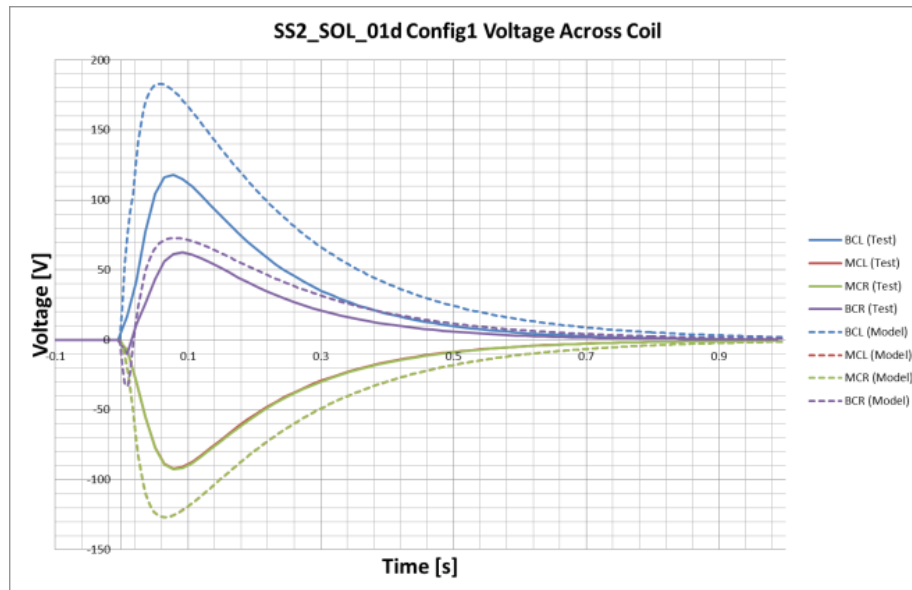


Fig. 4-4. Voltage across coils vs. time for Configuration 1. Test data (solid lines) and Model 2 result (dashed lines), second bucking coil quench developed after 12 ms.

These model results match much better with test data than the case of a single, initial quench. All the curves follow similar patterns, although the model still predicts more rapid current decay and more extreme voltages. In addition, the modeled voltage curves rise more quickly and peak sooner than the test curves (consistent with faster current decay). Therefore, the modeling program overestimates the severity of the quench, but the disparity partly originates from the unknown exact conditions of quench initiation in the real focusing lens. Moreover, the program cannot take into account all the factors present in a testing environment.

Fig. 4-7 illustrates the Model 2 prediction for how temperatures in the bucking coils develop as they quench, with the curves of the main coils staying constant at the operating temperature of 4.2 K. Given that the simulation overestimates the peak coil voltages, we conclude that the predicted peak temperatures are similarly conservative overestimates.

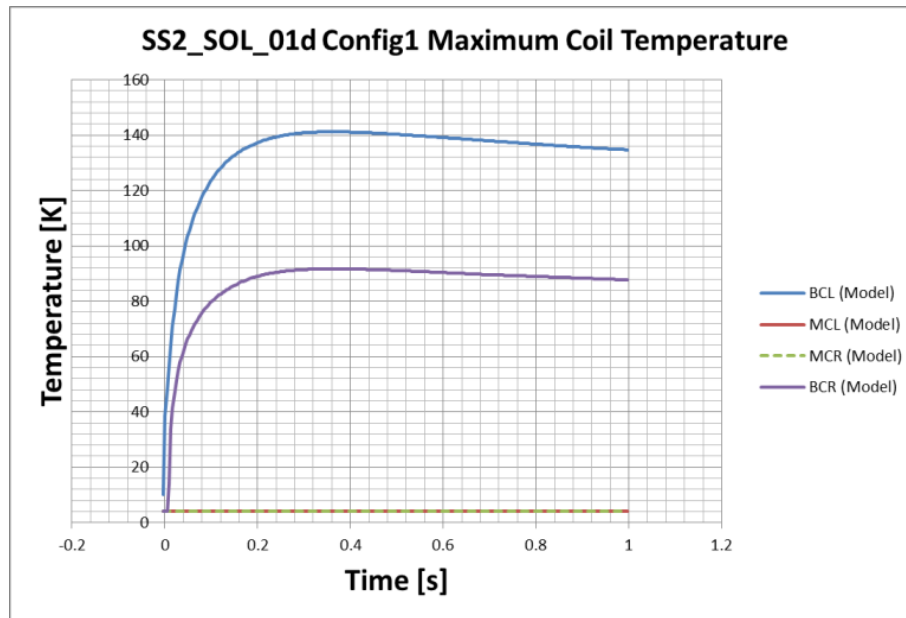


Fig. 4-7. Coil peak temperatures vs. time for Configuration 1, Model 2 result (second bucking coil quench developed after 12 ms).

4. B) Configuration 2: 1 Ohm Resistors in Parallel with Main Coils and 3 Ohm Resistors in Parallel with Bucking Coils

All of the quench events for this circuit configuration follow the same current and voltage development pattern, albeit at different initial currents. For analysis, quench #16 in BCL at 226.5 A was selected. Model 2 was run with a secondary quench started in the BCR 17 ms after the first quench in the BCL, based on the test voltage signals.

Once again, the test and model curves shown in Figures 4-8 and 4-9 follow similar trends. The initial current drop in the model is faster than that shown by the test. However, modeled current decay slows down significantly beginning around $t = 0.05$ s, though by $t = 0.3$ s it keeps pace with test results. This behavior is reflected in the voltage graphs. Notably, the model's voltages are again more extreme and grow faster than those of the test. Fig. 4-10 illustrates the Model 2 predictions for maximum temperature in each coil. Again, since the model yields higher voltages, the temperature calculations may be overestimations as well.

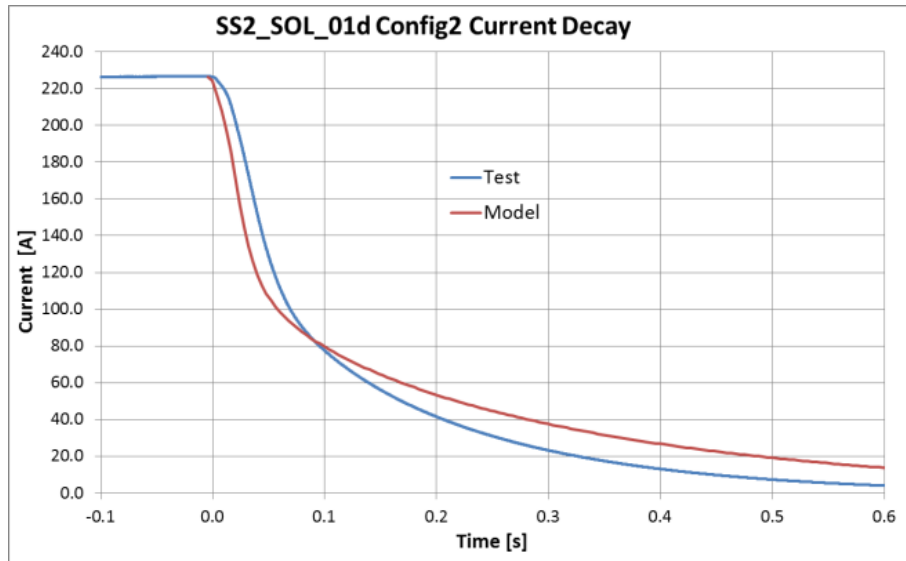


Fig. 4-8. Current vs. time for Configuration 2, Test data and Model 2 result (second bucking coil quench developed after 17 ms).

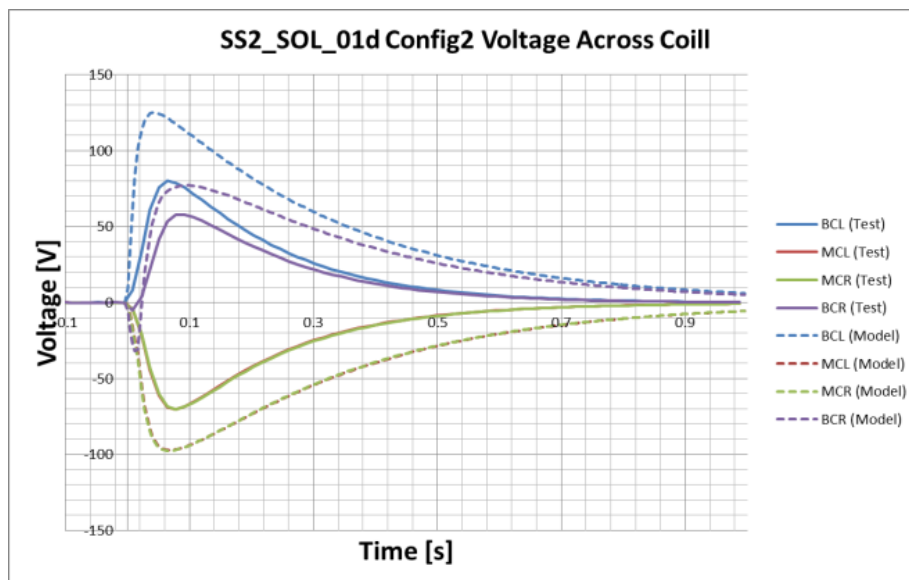


Fig. 4-9. Voltage across coils vs. time for Configuration 2. Test data (solid lines) and Model 2 result (dashed lines), second bucking coil quench developed after 17 ms.

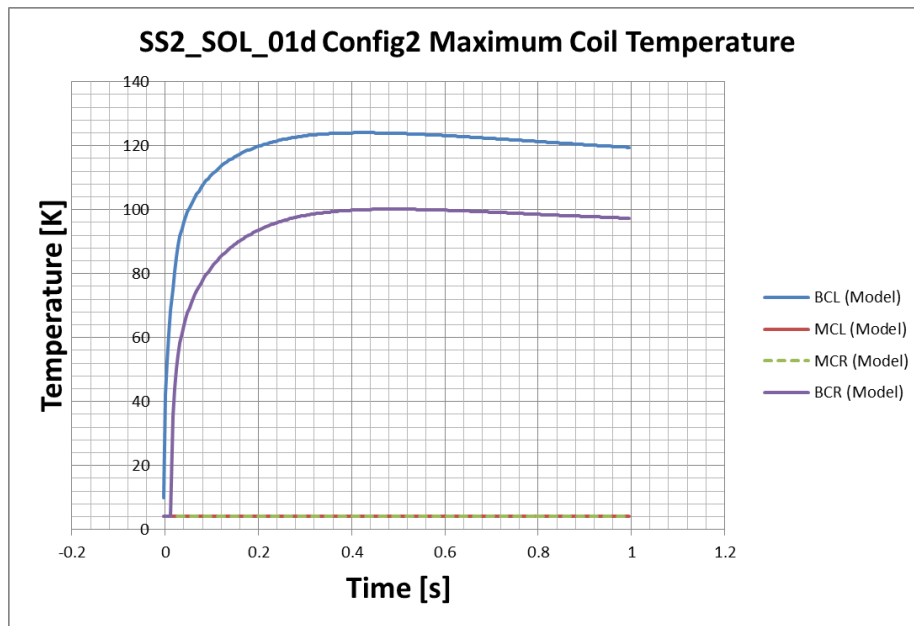


Fig. 4-10. Coil peak temperatures vs. time for Configuration 2, Model 2 result (second bucking coil quench developed after 17 ms).

4. C) Configuration 3: 3 Ohm Resistor in Series with Focusing Lens

Quench #33 occurred at a current of 205.7 A and the dump resistor was connected 10 ms after quench detection. Model 3 in this case specifies an initial quench in the lead end bucking coil followed by a quench in the return end bucking coil 16 ms later. Comparison of the current and voltage profiles are made in Figures 4-11 and 4-12 respectively, and the predicted coil temperatures are shown in Fig. 4-13.

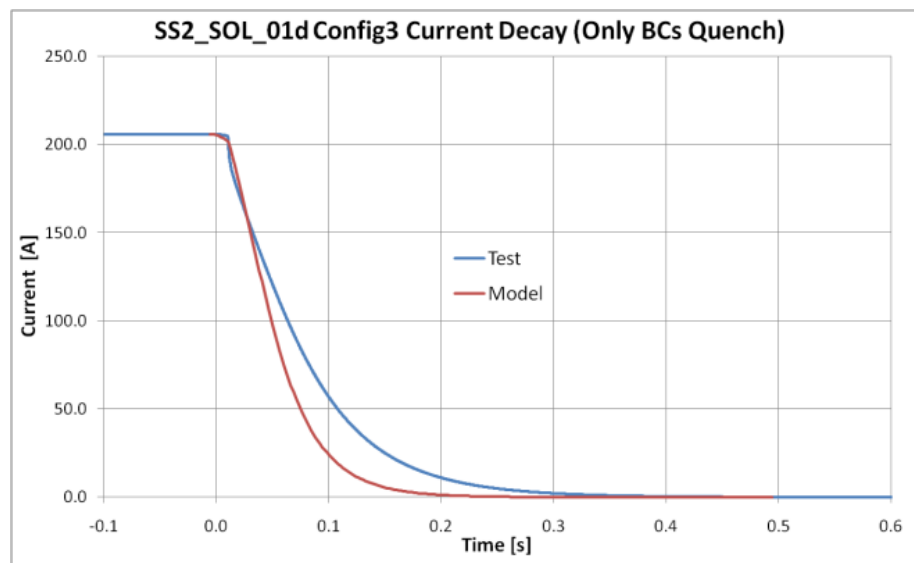


Fig. 4-11. Current vs. time for Configuration 3, Test data and Model 3 result (second bucking coil quench developed after 16 ms).

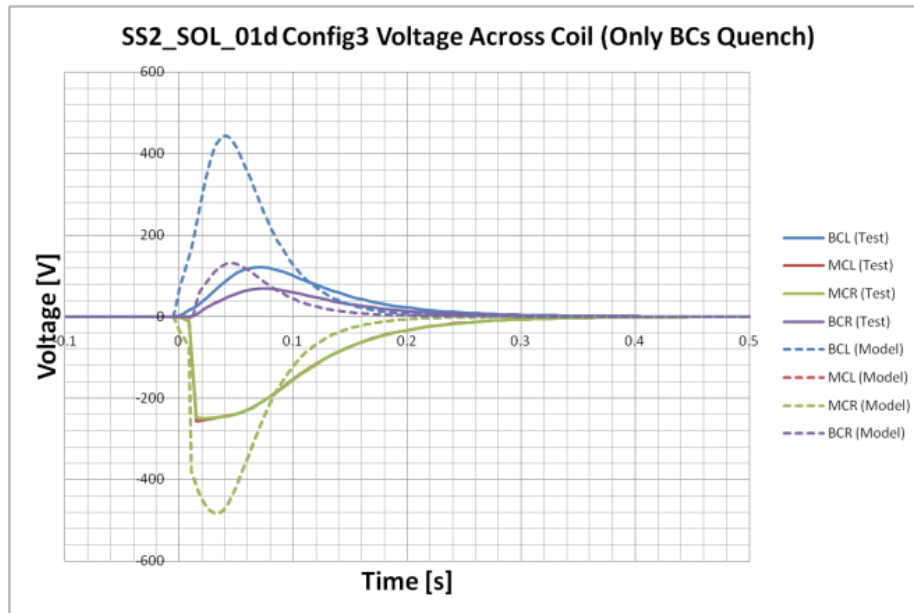


Fig. 4-12. Voltage across coils vs. time for Configuration 3. Test data (solid lines) and Model 3 result (dashed lines), second bucking coil quench developed after 16 ms.

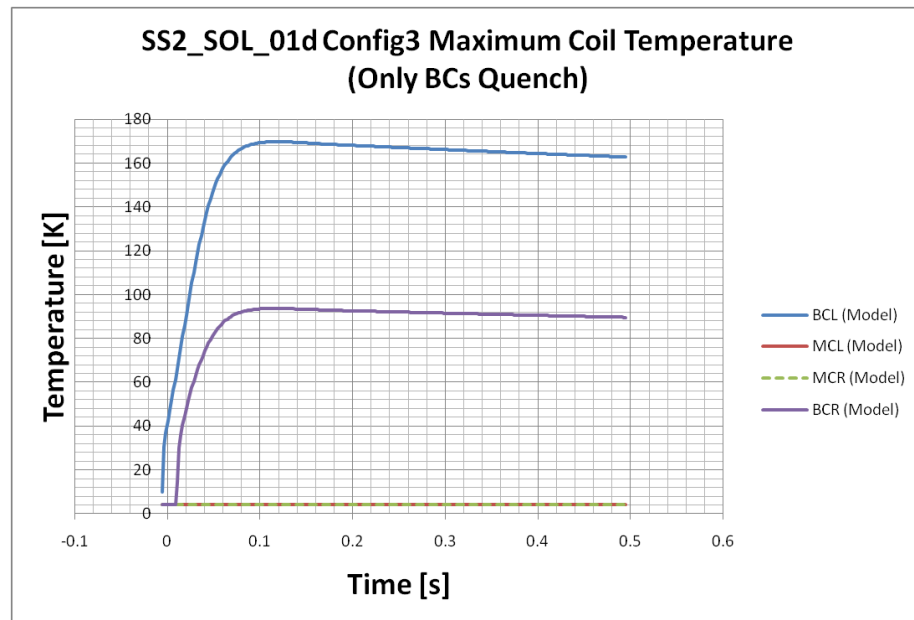


Fig. 4-13. Coil peak temperatures vs. time for Configuration 3, Model 3 result (second bucking coil quench developed after 16 ms).

Although the test and model graphs do not match up exactly, the curves follow similar patterns with deviations like those described earlier. In the model, current decays too rapidly and voltages across coils escalate more quickly to greater levels than those shown by the test – to about four times the peak voltage for the quenching BCL. One notable disparity can be seen in

the voltage across the main coils right after the dump is connected ($t=10$ ms). The model predicts continued voltage decrease, while the test results show that at that point the voltage begins to increase.

One possibility for this difference could be that all coils (not just the bucking coils) quench due to the sudden inclusion of the dump resistor in the circuit. A modified version of Model 3 was created to simulate this case, with the results shown in Figures 4-14, 4-15, and 4-16.

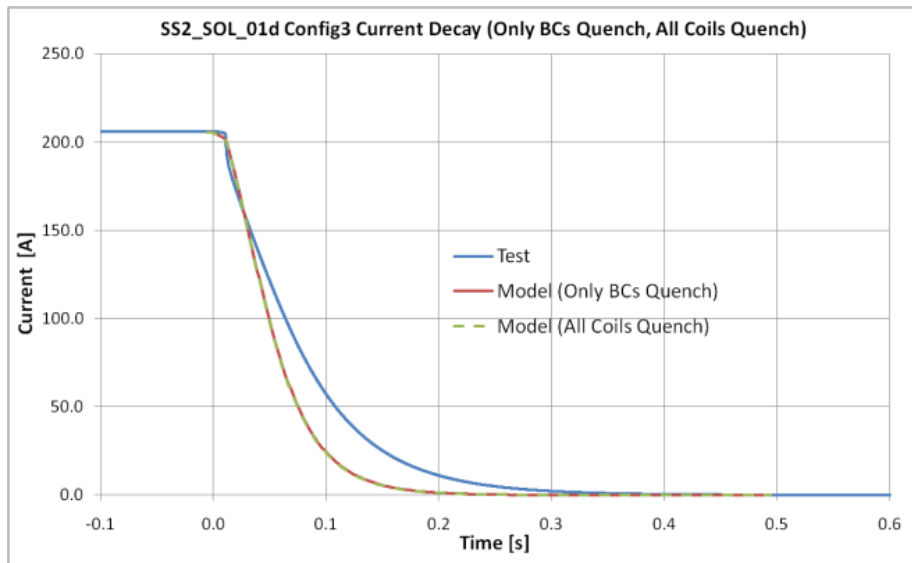


Fig. 4-14. Current vs. time for Configuration 3, Test data and modified Model 3 result, comparing case of both BCs quenching to case of all coils quenching.

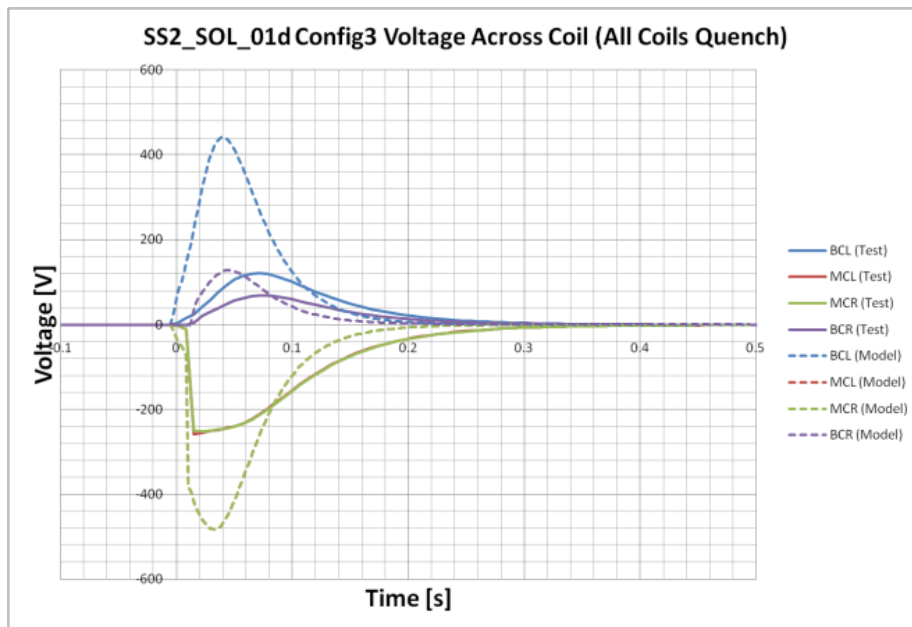


Fig. 4-15. Voltage across coils vs. time for Configuration 3. Test data (solid lines) and modified Model 3 result (dashed lines), in which second BC and both MCs quench after 16 ms.

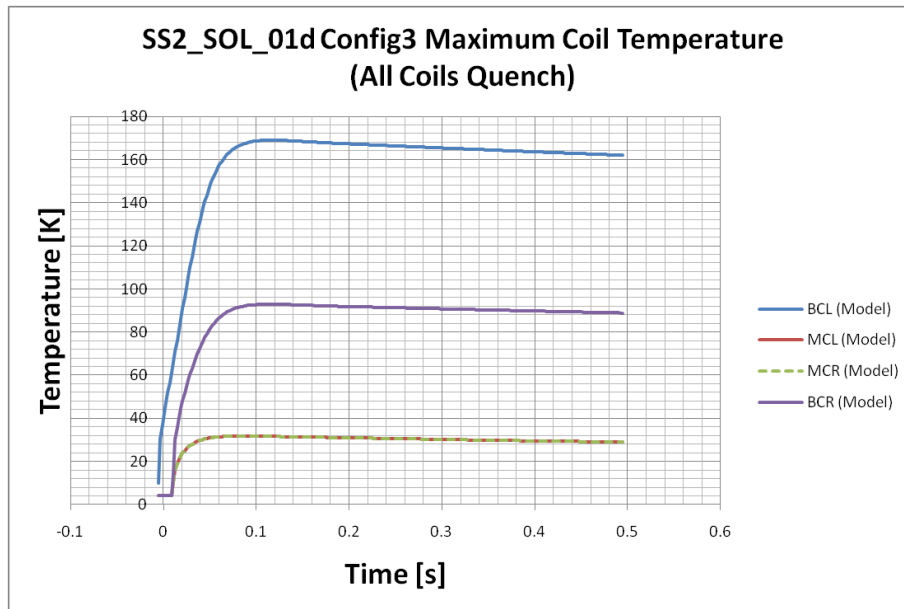


Fig. 4-16. Coil peak temperatures vs. time for Configuration 3, Model 3 result (second bucking coil quench developed after 16 ms).

Looking at Fig. 4-14, we can observe that the model's current curves for both quench scenarios are almost identical. The voltages in Fig. 14 and 17 likewise are equivalent. The lack of any significant change among the two cases indicates that the additional quenching of the main coils is not important. Fig. 4-16 supports this assertion by demonstrating that the maximum temperature in the main coils barely surpasses 30 K, meaning that the developed resistance is small. As a consequence, it may be hard to discern whether the main coils quench for any of the four configurations, but in the end this uncertainty does not really matter.

Since quenching main coils do not explain the behavior of the voltage across the main coils at $t=10$ ms, other factors such as inaccurate temperature, resistance or inductance calculations must be contributing to the disparity between test and model.

4. D) Configuration 4: No Protection

In the chosen case for this configuration, Quench #26, the return end bucking coil quenches initially and is followed by the other bucking coil after 57 ms, at a current of 180.0 A. To simulate no protection, Model 3 was employed with the series dump resistance set to 0. This configuration is the simplest of all the ones discussed, so the agreement between test and model can be most clearly examined. The previous trends of the model's more rapid current decay and quicker, greater voltage development are again visible in this case, shown in Figures 4-17, 4-18. As already mentioned, a possible explanation may be the unknown location of quenching. In the model, quenches are initiated in the location of greatest magnetic field, since this area is most likely to quench and studies show it leads to the most dangerous conditions in the system. However, two other locations were investigated: the outermost turn in the middle layer of the

bucking coil, and the area of lowest magnetic field. Furthermore, the size of the model's time step was reduced by ten to improve accuracy and then the initial case was modeled again. Fig. 4-17 displays the current decay curves of all the above variations. We can see that there is no significant difference in results. Likewise, voltage and temperature development will not really change. In the predicted (and over-estimated) temperature profile, shown in 4-19, the BCR reaches a peak temperature of 225 K which is high enough to be a concern.

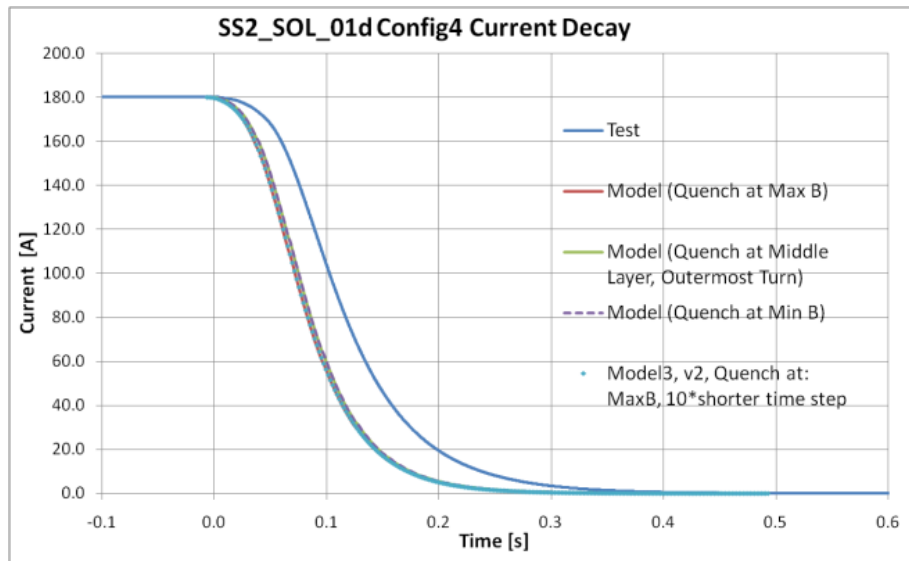


Fig. 4-17. Current vs. time for configuration 4. Test data and Model 3 predictions with quench initiation in varied locations, along with a shorter time step.

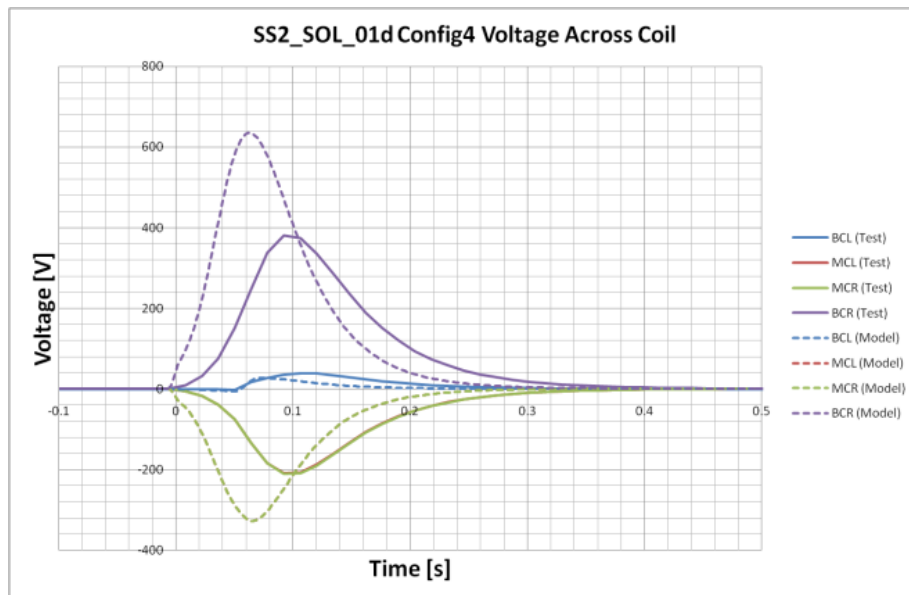


Fig. 4-18. Voltage across coil vs. time for configuration 4. Test data and Model 3 prediction with quench initiation in area of greatest magnetic field.

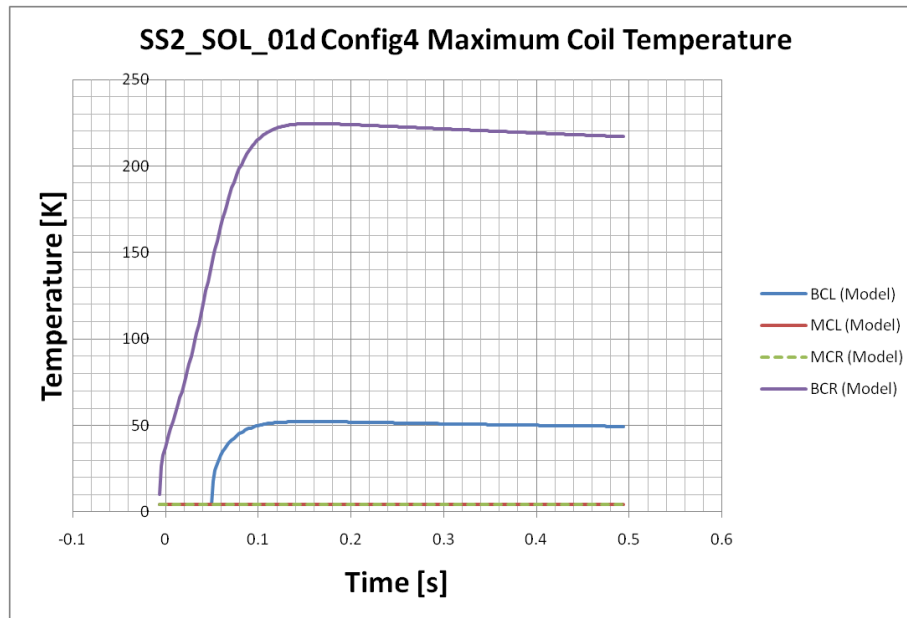


Fig. 4-19. Coil peak temperature vs. time for configuration 4. Model 3 prediction with quench initiation in area of greatest magnetic field.

4. E) Error Analysis

Since the computer models cannot take into account all the factors present in a physical system, it is not surprising that there exist deviations between predictions and test data. Moreover, the actual quench conditions (e.g. location and time of initiation) are not known exactly and have to be approximated. Many other unknowns exist, like the temperature distribution in the lens before and during quenching. The models also make substantial use of approximations in order to speed up computation, which leads to inaccuracy. The test results themselves could suffer from uncertainties in the experimental conditions in a complex system, especially given the difficulties with power and dump switch encountered during the test.

Differences in current decay and the high voltages may also be attributed to uncertainties in the derived values for inductances in the magnetic system, which play a major role in calculations. For example, eddy currents likely develop in the flux return surrounding the lens, causing a distorted magnetic field and consequently different inductances. This behavior is not considered in the models. In addition, the exact behavior of materials, especially at low temperatures, is uncertain. An overestimation in voltage could result from an overestimation in coil resistance. Moreover, material properties determine quench velocity and thus, developed resistance.

Nonetheless, the models consistently predict more dangerous conditions than those seen in real quenches. Additional modeling was made and compared to data at lower currents to systematically explore the trends of voltage and temperature; the following tables 4-1 through 4-4 illustrate how predictions scale with initial current and how they compare with test results, for each of the quench protection configurations.

Table 4-1. Config. 1 comparison of voltage data from test and model 2. Format is test/model.

| Initial Current (A) | Max. Voltage across first quenching BC (V) | Max. Voltage across each MC (V) | Max. Voltage across second BC (V) |
|---------------------|--|---------------------------------|-----------------------------------|
| 78.1 | 27 / 43 = 0.63 | -14 / -21 = 0.67 | -2 / -4 = 0.50 |
| 147.4 | 75 / 114 = 0.66 | -51 / -73 = 0.70 | 22 / 32 = 0.69 |
| 208.1 | 118 / 183 = 0.64 | -92 / -127 = 0.72 | 63 / 73 = 0.86 |
| Average | 0.64 | 0.70 | 0.78 |

Table 4-2. Config. 2 comparison of voltage data from test and model 2. Format is test/model.

| Initial Current (A) | Max. Voltage across first quenching BC (V) | Max. Voltage across each MC (V) | Max. Voltage across second BC (V) |
|---------------------|--|---------------------------------|-----------------------------------|
| 170.0 | 57 / 84 = 0.68 | -44 / -64 = 0.69 | 31 / 48 = 0.65 |
| 226.5 | 80 / 125 = 0.64 | -70 / -98 = 0.71 | 58 / 77 = 0.75 |
| 241.8 | 77 / 150 = 0.51 | -78 / -105 = 0.74 | 66 / 77 = 0.86 |
| Average | 0.61 | 0.71 | 0.75 |

Table 4-3. Config. 3 comparison of voltage data from test and model 3. Format is test/model.

| Initial Current (A) | Max. Voltage across first quenching BC (V) | Max. Voltage across each MC (V) | Max. Voltage across second BC (V) |
|---------------------|--|---------------------------------|-----------------------------------|
| 200.2 | 70 / 212 = 0.33 | -234 / -383 = 0.61 | 65 / 197 = 0.33 |
| 205.7 | 121 / 444 = 0.27 | -258 / -483 = 0.53 | 68 / 130 = 0.52 |
| 216.1 | 145 / 502 = 0.29 | -272 / -535 = 0.51 | 87 / 161 = 0.54 |
| Average | 0.30 | 0.55 | 0.46 |

Table 4-4. Config. 4 comparison of voltage data from test and model 4. Format is test/model.

| Initial Current (A) | Max. Voltage across first quenching BC (V) | Max. Voltage across each MC (V) | Max. Voltage across second BC (V) |
|---------------------|--|---------------------------------|-----------------------------------|
| 112.1 | 124 / 193 = 0.64 | -63 / -96 = 0.66 | 4 / -2 = -2.00 |
| 148.5 | 246 / 396 = 0.62 | -133 / -197 = 0.68 | 16 / 15 = 1.07 |
| 180.0 | 383 / 635 = 0.60 | -213 / -328 = 0.65 | 40 / 28 = 1.43 |
| Average | 0.62 | 0.66 | 1.25 |

We see that the actual peak voltages consistently have values about two thirds of those predicted by the models for every configuration except the third; in Table 4-3, the test results showed considerably lower voltages, about one third to one half of the predicted values.

The notable ratio between test and model data provides evidence that inductance, resistivity, or some other property of the system may have been overestimated by a constant factor. The model can provide some guidance about the relationship between temperature and voltage, and allows us to estimate (by scaling to the observed voltages) what the actual coil temperatures may be. In Fig. 4-20 we show the peak coil temperature versus the peak coil voltage, for the 1st and 2nd quenching BC, with one point for each test configuration (the highest

current case for each); Configuration 3 points are highlighted and suggest a slightly different trend. For the worst case configuration 4, the actual peak voltage of 383 V translates into an estimated peak temperature of 185 K, rather than 225 K.

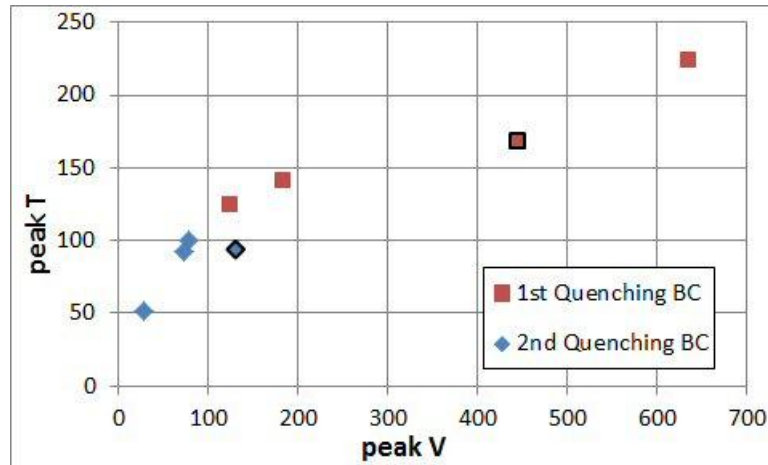


Fig. 4-20. Peak Temperature vs. Peak Voltage from the four modeled configurations at the highest current; highlighted points are configuration 3, which shows a slightly different trend.

4. F) Inductance Analysis

Calculations for inductances in solenoids (which make up the focusing lens) are described in [6]. The quench propagation models implemented the derived values for the SSR2 system. Total circuit inductance was calculated as 0.352 H. By analyzing the test data presented above, we can estimate the actual circuit inductance. Configuration 3 represents a simple LR circuit with a variable resistance, described by the following differential equation,

$$L * \frac{di}{dt} + R * i = 0 \quad /1/$$

We assume the circuit inductance L is dominated by the solenoid; R is the total resistance of the circuit, i is the current, and di/dt is the rate of current change. The circuit resistance is $R=R_d+R_c$, where R_d is the dump (plus copper bus) resistance, and R_c is the coil resistance which grows as the quench develops. In quench #33, the coil developed 2 V when detected at 205A, for a .01 Ω resistance, and the measured linear voltage growth rate gives 4 m Ω /ms rate of resistance growth. Thus R_c is negligible (1% effect) compared to the dump resistance $R_d=3 \Omega$ when the dump fires at 10 ms. Therefore using the measured $di/dt = -2062A/s$ just after the dump fired, we can estimate the solenoid inductance to be $L = -R_d/(di/dt) = 0.299$ H. This is slightly smaller than the calculated 0.352 H value, which corresponds to the DC inductance; we expect the inductance to decrease at higher frequencies.

4. G) Optimal Quench Protection Configuration

The data in Tables 4-1 to 4-4 confirm the conclusion of earlier protection modeling studies [3-5, 7] that Configuration 2 provides the best option for quench protection. Voltages across coils are well-balanced and stay at levels well below the hipot limit of 500 V, and tend to be lowest of the studied configurations. Consequently, energy dissipation would be more evenly balanced and conditions such as peak temperature would also be lower for Configuration 2.

5. Modeling Temperature Decay

Having observed somewhat erratic quench behavior, it was of interest to estimate how quickly the temperature of a quenched coil returns to base operating conditions. The following graphs were generated by allowing the quench simulation (model 3) to continue calculating the coil temperatures for two cases of a quenched bucking coil. Cooling of a quenched main coil should follow similar trends. Because of material properties at low temperatures, the temperature decay appears fairly linear throughout and is complete in much less than a minute. Fig. 5-1 and 5-2 show the same rate of about -4.5 K/s.

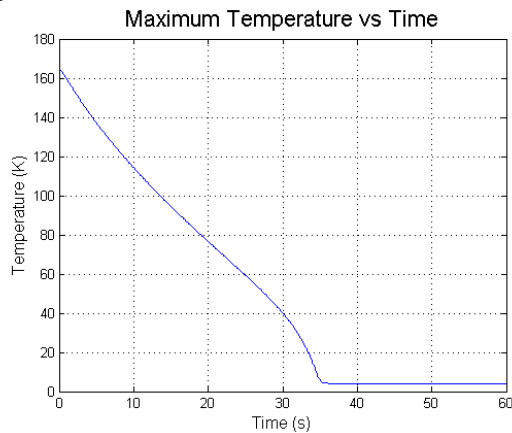


Fig. 5-1. Maximum temperature vs. time. Initial peak temperature of 165 K. Model 3 data.

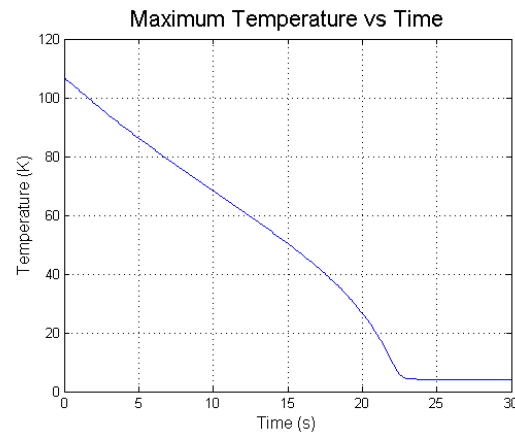


Fig. 5-2. Maximum temperature vs. time. Initial peak temperature of 107 K. Model 3 data.

6. Magnetic Measurements

Two aspects of the solenoid magnetic field have been considered: first, detailed study of the solenoid axis is in progress to assess the alignment of individual coils during construction, and to establish the level of stability in the axis position resulting from thermal cycling between room temperature and liquid helium temperatures. This ongoing program is quite elaborate and therefore deserves to be reported in a separate note once completed. The second area of interest is mapping the magnetic field profiles of the solenoid and dipole corrector coils, comparing to predictions and determining the field integrals. Due to the small solenoid aperture, a warm bore could not be used; therefore measurements were made along a geometrically centered axis, using axial and transverse cryogenic Hall probes from Cryomagnetics, Inc.

Related to earlier studies of fringe field reduction near SRF cavity walls, in this test a plate of Niobium was positioned at the Return End of the SS2 solenoid, to measure its

effectiveness as a Meissner shield to attenuate the fringe field. The 100mm x100 mm square plate was 2 mm thick, with a 36 mm center hole for mounting around the Hall probe guide tube. The plate was located 35 mm from the solenoid return end, or 165 mm from the center.

The solenoid field was mapped at 200 A on March 12 after reaching the maximum quench current; first the entire field profile was measured, then fine scans around the ends were made to measure the fringe fields in detail. The results are shown in Figures 6-1, 6-2, and 6-3; the overall agreement with expectations is good. In the fringe field region the asymptotic values agree with the model, but the transition regions differ somewhat from each other and from the model. The measured return end field is much lower than at the lead end, but it is not necessarily due to the Nb Meissner shield: deviation of the BC from the nominal position can also influence the detailed field shape in this region – further modeling should be made to predict how the end field shape is modified by this plate, or by BC position, before conclusions can be drawn here.

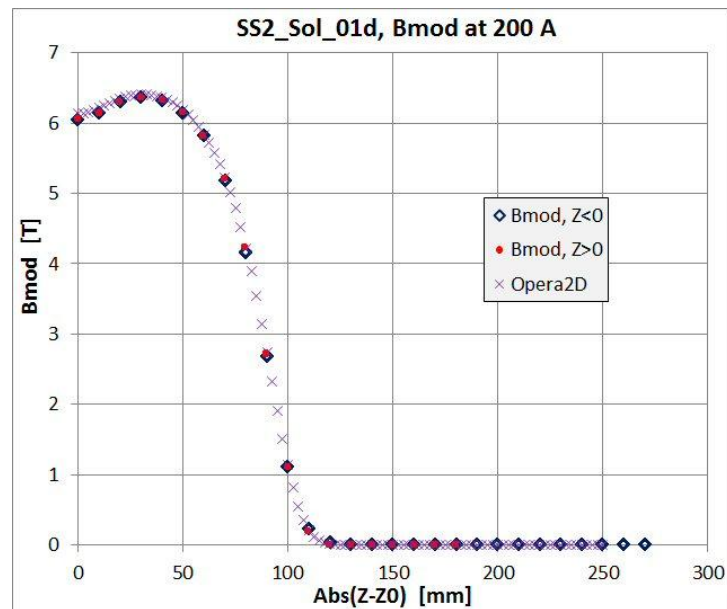


Fig. 6-1. The solenoid axial field profile is shown with as-built Opera2D model prediction showing very good agreement and symmetry about the center. Positive Z is the top (LE) and negative Z is the bottom (RE) of the solenoid.

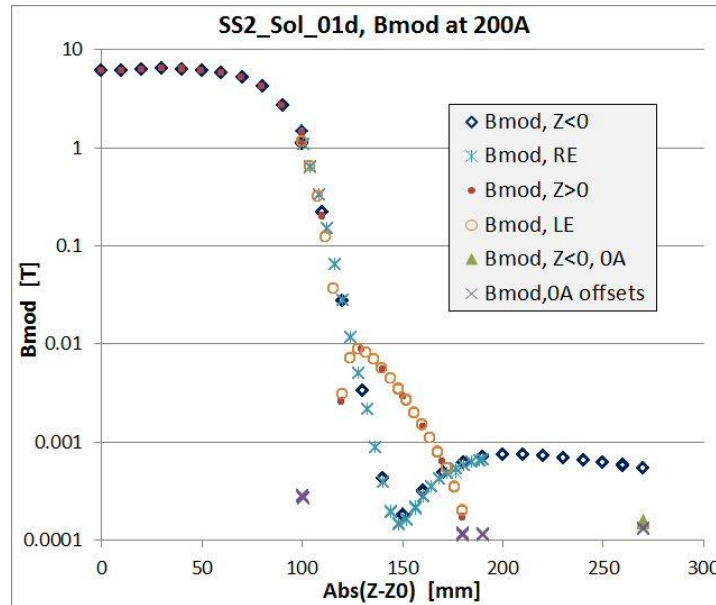


Fig. 6-2. The solenoid axial field profile is shown on a log scale to highlight the end field measurements; Bmod (total field magnitude) is plotted due to the axial field changing sign. Several measurements of the zero-current offset field values are also plotted to illustrate the background field level.

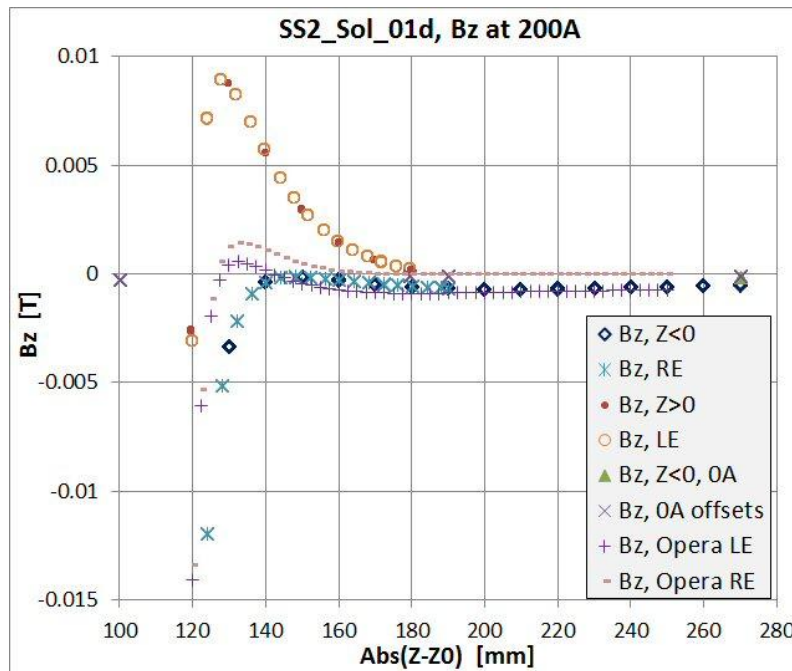


Fig. 6-3. The solenoid axial field profiles for both ends are shown with Opera2D as-built predictions for comparison; Nb plate at Return End (165 mm) was not modeled.

The dipole correctors were powered in series at 100 A and measured on March 15, after adjusting the transverse probe orientation to maximize the central field reading; Fig. 6-4 shows

the profile. From this graph the field integral BL for each dipole is approximately $B_p L / \sqrt{2}$, assuming they have identical strengths, where $B_p = 0.267$ T and $L = 0.17$ m, or $BL = 0.032$ T-m at 100A. Since the dipoles quench in the 200A solenoid field at 47.8 A, the maximum achievable bending field under nominal operating conditions is about 1.5 T-cm for each dipole.

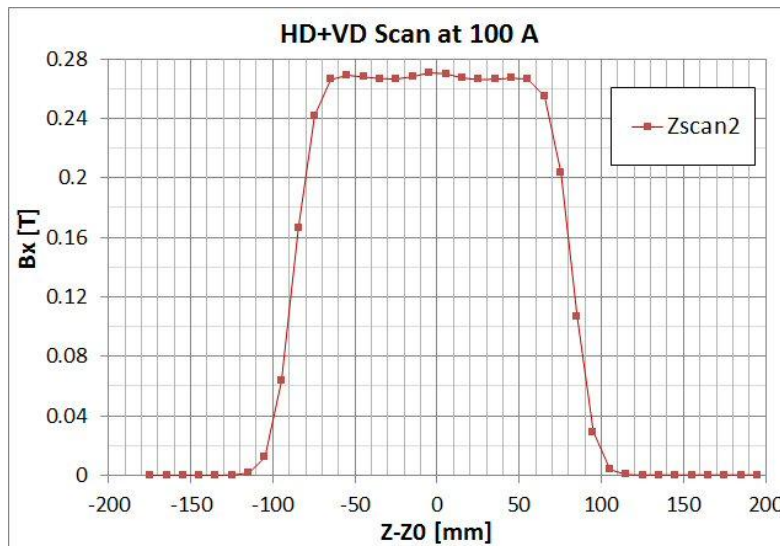


Fig. 6-4. The transverse field profile for both steering dipoles in series at 100 A.

7. Summary

The prototype SS2 solenoid was quench tested in 4.4 K liquid helium and exhibited relatively slow training and some erratic quench behavior; although it reached the expected maximum quench current, a plateau at maximum current was not maintained. After the test it was found that several bolts supporting the yoke against axial forces had become loose; this could certainly explain the erratic quench behavior, and it is possible that repeated shocks from the slow training caused the bolts to loosen.

Because this solenoid has large stored energy, studies suggested the quenching coils can experience dangerously high voltages and temperatures. Therefore the main purpose of the test was to evaluate the effectiveness of several different quench protection schemes, and compare the actual behavior to simulations that were used to optimize the configuration for solenoid protection. Four separate configurations of energy extraction resistors were tested and compared to simulations, including the case of full energy absorption with no external protection resistor.

For all of these configurations, the quench propagation models safely overestimate the severity of conditions in the SSR2 focusing lens during quenching, but predict behaviors comparable to the experimental data (coil voltages and total current). The overestimation of voltages across coils tends to be approximately a factor of 1.5, although in the case of a simple dump resistor across the entire magnet, it is a factor 2 to 3 high. Test and model results show that peak voltages scale linearly with quench current. In general the model predicts faster voltage rise and current decay than is observed, consistent with overestimation of the peak voltages.

Inaccurate coil resistance and/or inductance calculations probably contribute to most of the error. Nevertheless the model provides a useful analytical tool to examine the thermal and electrical characteristics of a quenching magnet system, and a number of refinements to the model may be introduced that can be checked against the SS2 quench data:

- Making inductance depending on frequency f , performing actual $L(f)$ measurements
- Making a better approximation for thermal conductivity of the strand and of the composite
- Taking into account that the quench starts at a point, not on a line: making a true 3D model.

Although the solenoid survived high current quenches without protection, it reached a rather high peak voltage of 383 V, and an estimated peak temperature of 175 K. Therefore protection must be implemented to ensure safe and reliable operation. Both the test data and model results suggest that the optimal configuration for quench protection, out of the three analyzed, consists of 1 ohm resistors connected in parallel with main coils and 3 ohm resistors connected in parallel with bucking coils. The other configurations with fewer resistors also seem adequate, although their protection is not as effective. In any case, the bucking coils must be more carefully protected because testing demonstrates that they quench much more frequently than the main coils and more easily develop high voltages.

The thermal modeling was extended to predict the temperature trend following a fully quenched bucking coil. The model indicates that cooling proceeds at an approximately constant rate of -4.5 K/s. Therefore, most quenched systems comparable to the SSR2 bucking coil should be able to return to operating temperature in less than a minute.

Magnetic measurements of the solenoid and dipole field profiles along the axis were made. The solenoid field is in very good agreement with model predictions, both in the body and fringe field regions. The maximum dipole integral strength, which corresponds to the dipole quench current in the solenoid field operating at 200 A, is approximately 1.5 T-cm.

8. References

- [1] G. Davis, et al., "HINS Linac SS2 Section Prototype Focusing Lens Design," TD-09-003, Jan. 27, 2009.
- [2] S. Nagaitsev, et al., "PXIE: ProjectX Injector Experiment," IPAC-2012, THPPP058 (2012)
- [3] E. Khabiboulline and I. Terechkine, "SSR2 Focusing Lens Quench Protection Study: Dump Resistors Connected in Parallel to Coils of the Lens," TD-11-006, Apr. 06, 2011.
- [4] E. Khabiboulline and I. Terechkine, "Modeling Quench Propagation in Inductively Coupled System of Coils: Dump Resistors Connected in Parallel to Each Coil in the System," TD-11-011, Aug. 22, 2011.
- [5] E. Khabiboulline and I. Terechkine, "Quench Protection of SSR-2 Focusing Lens: Resistors Connected to All Coils of the Lens," TD-11-018, Sep. 26, 2011.
- [6] E. Khabiboulline, "Quench Protection of Focusing Lenses for PXIE Cryomodules," TD-12-002, Mar. 19, 2012.
- [7] I. Terechkine, "SS2 Focusing Solenoid Quench Protection Study," TD-09-016, June 2009.